ELSEVIER

Journal of Organometallic Chemistry 633 (2001) 114–124

Journal of Organometallic Chemistry

www.elsevier.com/locate/jorganchem

Organometallic complexes for nonlinear optics[☆] Part 23. Quadratic and cubic hyperpolarizabilities of acetylide and vinylidene complexes derived from protected and free formylphenylacetylenes

Stephanie K. Hurst [a], Nigel T. Lucas [a], Marie P. Cifuentes [a], Mark G. Humphrey [a,*], Marek Samoc [b], Barry Luther-Davies [b], Inge Asselberghs [c], Roel Van Boxel [c], André Persoons [c]

[a] *Department of Chemistry, Australian National University, Canberra, Australian Capital Territory 0200, Australia*
[b] *Laser Physics Centre, Research School of Physical Sciences and Engineering, Australian National University, Canberra, Australian Capital Territory 0200, Australia*
[c] *Laboratory of Chemical and Biological Dynamics, Centre for Research on Molecular Electronics and Photonics, University of Leuven, Celestijnenlaan 200D, B-3001 Leuven, Belgium*

Received 18 April 2001; accepted 20 June 2001

Abstract

The acetylenes 4-HC≡CC_6H_4R [R = CH{OC(O)Me}$_2$ (**1**), $\overline{CHO(CH_2)_3O}$ (**2**)], ruthenium complexes [Ru(4-C≡CC_6H_4R)(PPh_3)$_2$-(η-C_5H_5)] [R = CH{OC(O)Me}$_2$ (**3**), CHO (**4**)], [Ru(*n*-C=CHC_6H_4R)Cl(dppm)$_2$]PF_6 [*n* = 4, R = $\overline{CHO(CH_2)_3O}$ (**7**); R = CHO, *n* = 3 (**11**), 2 (**15**)], and [Ru(*n*-C≡CC_6H_4R)Cl(dppm)$_2$] [*n* = 4, R = $\overline{CHO(CH_2)_3O}$ (**8**); *n* = 3, R = CHO (**12**)], and gold complexes [Au(*n*-C≡CC_6H_4R)(L)] [*n* = 4, R = CHO, L = PPh_3 (**5**), PMe_3 (**6**); *n* = 4, R = $\overline{CHO(CH_2)_3O}$, L = PPh_3 (**9**), PMe_3 (**10**); *n* = 3, R = CHO, L = PPh_3 (**13**), PMe_3 (**14**)] have been prepared, and **9** characterized by a single crystal X-ray diffraction study. Electrochemical data for the ruthenium complexes reveal reversible or quasi-reversible (alkynyl complexes) or irreversible (vinylidene complexes) processes assigned to the $Ru^{II/III}$ couple; the effect on $E_{1/2}$ values of the various structural modifications across **3**, **4**, **7**, **8**, **11**, **12** and **15** are discussed. The molecular quadratic and cubic optical nonlinearities of **1**–**15** have been determined by the hyper-Rayleigh scattering technique at 1064 nm and the *Z*-scan technique at 800 nm, respectively; β values increase on increasing the acceptor strength, proceeding from 3-acceptor-substituted to 4-acceptor-substituted arylalkynyl ligand, and an increasing phosphine donor strength, whereas γ values increase on increasing the number of phosphine aryl groups (i.e. increasing delocalization) proceeding from PMe_3 to PPh_3-containing complex. © 2001 Published by Elsevier Science B.V.

Keywords: Ruthenium; Gold; Hyperpolarizability; Acetylide; Vinylidene; Electrochemistry; X-ray structure

1. Introduction

The optical nonlinearities of organometallic complexes have commanded significant recent interest [2–4]. The particular target of our nonlinear optical (NLO) studies has been ruthenium and gold acetylide complexes [5–17], but our previous reports have largely focused on nitroarylalkynyl complexes, for which significant quadratic and cubic NLO coefficients have been observed. Replacing the strong nitro acceptor by an aldehyde functionality would be expected to reduce nonlinearities, but would provide a functional group which could be utilized to build more extended structures. Our attention has therefore recently turned to formylphenylalkynyl ligands. We report herein syntheses of a range of vinylidene and alkynyl complexes containing such ligands, synthetic procedures to prepare and introduce 1,3-dioxane and geminal diacetate-protected formyl groups onto such ligands, and studies

[☆] Part 22: see Ref. [1].

* Corresponding author. Tel.: +61-2-6125-2927; fax: +61-2-6125-0760.

E-mail address: mark.humphrey@anu.edu.au (M.G. Humphrey).

0022-328X/01/$ - see front matter © 2001 Published by Elsevier Science B.V.
PII: S0022-328X(01)01077-4

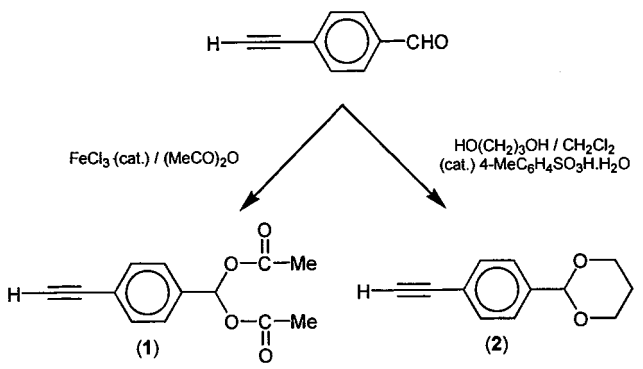

Scheme 1. Syntheses of **1** and **2**.

of the electrochemical, quadratic and cubic NLO properties of the resultant complexes.

2. Results and discussion

2.1. Synthesis and characterization of terminal acetylenes

Arylacetylenes with a protected formyl group were required for the subsequent preparation of alkynyl complexes. 4-HC≡$CC_6H_4CH\{OC(O)Me\}_2$ (**1**) was prepared by extending the method of Kochar et al. [18], stirring 4-HC≡CC_6H_4CHO in acetic anhydride with a catalytic amount of $FeCl_3$ (Scheme 1). The formyl group can also be protected by conversion into a 1,3-dioxane moiety. This was accomplished by stirring 4-HC≡CC_6H_4CHO in a mixture of dichloromethane and 1,3-propanediol with a catalytic amount of 4-toluenesulfonic acid monohydrate, to give **2** in good yield (Scheme 1). While the current research was in progress, synthesis of **2** was reported by acetalizing 4-Me_3SiC≡CC_6H_4CHO with 1,3-propanediol, and desilylating the intermediate with K_2CO_3–methanol, although the yield by this procedure was not specified [19]. The identities of **1** and **2** were confirmed by IR, UV–vis and ^{1}H-NMR spectroscopy, mass spectrometry (including accurate mass determinations of the molecular ion signal), and satisfactory microanalyses.

2.2. Synthesis and characterization of σ-acetylide and vinylidene complexes

The synthetic methodologies used in the preparation of the new complexes are adaptations of those utilized successfully in the preparation of the corresponding phenylacetylides. The bis{bis(diphenylphosphino)-methane}ruthenium complexes were prepared by extending the method of Touchard et al. [20], a procedure which also permits the isolation of the stable vinylidene intermediates; we have previously utilized this procedure to prepare the corresponding 4-formylphenyl-ethynyl and -vinylidene complexes [1] (Scheme 2). The behavior of the 2-formylphenylvinylidene complex **15** was markedly different, with attempted deprotonation resulting in decomposition. Unlike the analogous *trans*-[Ru(4-C≡CC_6H_4CHO)Cl(dppm)$_2$], it did not prove possible to prepare [Ru(4-C≡CC_6H_4CHO)$(PPh_3)_2(\eta$-$C_5H_5)$] by the most direct route, namely reaction of [RuCl-$(PPh_3)_2(\eta$-$C_5H_5)$] with 4-HC≡CC_6H_4CHO followed by basic work-up; only decomposition products were observed. Access to the 4-formylphenylethynyl complex necessitated the preparation of a complex with a protected formyl group. The (cyclopentadienyl)bis(triphenylphosphine)ruthenium acetylide complex **3**, containing a protected formyl group, was prepared in good yield by the reaction of **1** with [$RuCl(PPh_3)_2(\eta$-$C_5H_5)$] and deprotonation of the intermediate vinylidene complex. Deprotection of **3** by extended treatment with base afforded the formylphenylethynyl complex **4** in good yield (Scheme 3). Gold acetylide complexes containing 3-formyl, 4-formyl or 4-(1,3-dioxane) substituents at the phenylethynyl ligand were prepared

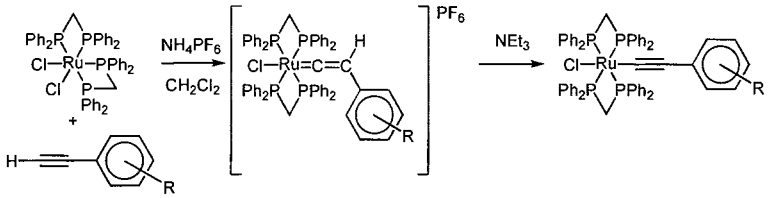

R	Complex	Ref
4-CHO(CH$_2$)$_3$O	7	This work
3-CHO	11	This work
2-CHO	15	This work
4-CHO		[1]

R	Complex	Ref
4-CHO(CH$_2$)$_3$O	8	This work
3-CHO	12	This work
4-CHO		[1]

Scheme 2. Syntheses of *trans*-bis{bis(diphenylphosphino)methane}chlororuthenium acetylide and vinylidene complexes.

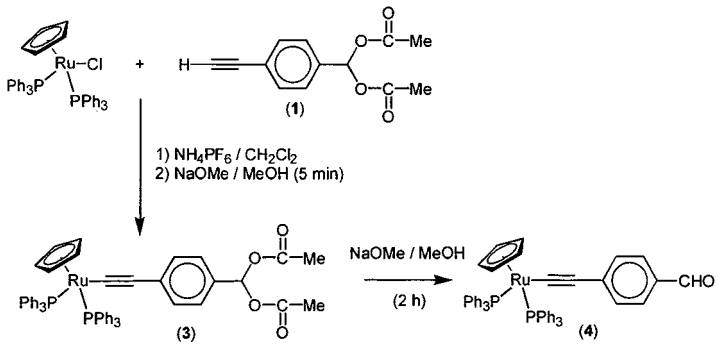

Scheme 3. Synthesis of complexes **3** and **4**.

in good yield by extending the method of Naulty et al. [15] (Scheme 4).

The new complexes were characterized by SI mass spectrometry, satisfactory microanalyses, UV–vis, IR, ^{1}H- and ^{31}P-NMR spectroscopy. Characteristic ν(C≡C) bands are found in the ranges of 2053–2081 and 2112–2120 cm^{-1} for the new ruthenium and gold alkynyl complexes, respectively, and ν(PF) bands are found at about 840 cm^{-1} for the PF_6^- salts of the vinylidene complex cations. The cyclopentadienyl ligand resonates as a sharp singlet in the ^{1}H-NMR spectra of **3** (4.29 ppm) and **4** (4.33 ppm). The ^{1}H-NMR spectra of the vinylidene complexes contain characteristic multiplets for RuC=C*H* at 2.95 (**7**), 3.13 (**11**) and 6.40 (**15**) ppm, the significant downfield shift observed in **15** presumably arises from chemical shift anisotropy effects of the 2-formyl group. The ^{31}P-NMR spectra of all complexes contain one singlet resonance, consistent with the molecular symmetry in the poly-phosphine complexes. The UV–vis spectra for these alkynylmetal complexes contain MLCT bands at low energy; for the gold complexes, replacing alkynyl substituent CHO by $\overline{CHO(CH_2)_3O}$ results in a shift to higher energy, as does replacing 4-CHO by 4-CH{OC(O)Me}$_2$ for the ruthenium complexes in proceeding from **4** to **3**. The 2-formylphenylvinylidene complex **15** is unusual in possessing a much lower energy λ_{max} (555 nm); this unique band may result from the interaction between the vinylidene proton and the formyl oxygen, hydrogen bonding between which forms a six-membered ring. Support for this possibility can be seen in the ^{13}C-NMR chemical shifts of the formyl carbons [170.2 ppm (**15**), cf. 191.9 ppm (**12**), 191.2 ppm (**4**)]

2.3. X-ray crystallographic study

The identity of **9** was confirmed by a single-crystal X-ray diffraction study. Crystal data are given in Table 1 and selected bond lengths and bond angles are compiled in Table 2. Fig. 1 contains an ORTEP plot showing the molecular geometry and atomic labeling scheme.

Intraphosphine bond lengths and bond angles in **9** are not unusual. The Au–P, Au–C(1) and C(1)–C(2) bond distances are within the range of the values observed earlier for (phosphine)gold acetylide complexes [11,21]. Angles about the P–Au–C(1)–C(2) moiety are close to linearity, with any deviations likely to be the result of crystal packing forces. Distances within the phenyl and 1,3-dioxane components of the alkynyl ligand are not unexpected. Gold complexes have attracted significant interest as many show aurophilic Au···Au interactions in the solid state. In the present case, though, there are no Au···Au contacts < 5 Å.

2.4. Electrochemical studies

The results of cyclic voltammetric investigations into the new ruthenium acetylide complexes are summarized in Table 3 together with data reported earlier for related complexes. All new complexes show an anodic wave assigned to the $Ru^{II/III}$ oxidation process. The tabulated data are consistent with several broad trends. Alkynylruthenium complexes exhibit reversible or quasi-reversible processes (in the range of 0.51–0.67 V for the new complexes), whereas the vinylidene complexes exhibit irreversible complexes at a considerably more positive potential (the latter as expected for cationic complexes). The 2-formylphenylvinylidene

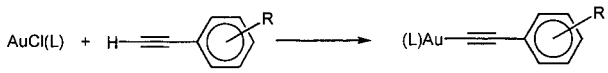

L	R	Complex
PPh_3	4-CHO	**5**
PMe_3	4-CHO	**6**
PPh_3	4-$\overline{CHO(CH_2)_3O}$	**9**
PMe_3	4-$\overline{CHO(CH_2)_3O}$	**10**
PPh_3	3-CHO	**13**
PMe_3	3-CHO	**14**

Scheme 4. Synthesis of (phosphine)alkynyl gold complexes.

Table 1
Crystallographic data and structure refinement parameters for complex **9**

Empirical formula	$C_{30}H_{26}AuO_2P$
Formula weight	646.47
Temperature (K)	200
Wavelength (Å)	0.71069
Crystal system	Monoclinic
Space group	$P2_1/a$ (No. 14)
Unit cell dimensions	
a (Å)	13.8579(2)
b (Å)	12.2231(1)
c (Å)	14.9604(2)
β (°)	96.492(7)
V (Å^3)	2517.84(6)
Z	4
Absorption coefficient (mm^{-1})	5.952
Crystal size (mm)	$0.30 \times 0.25 \times 0.20$
Theta range for data collection (°)	2.96–30.07
Index ranges	$-19 \le h \le 19$, $-17 \le k \le 17$, $-21 \le l \le 21$
Reflections collected	66 569
Independent reflections	7701 ($R_{int} = 0.077$)
Max/min transmission	0.222, 0.384
Data/restraints/parameters	5733/0/307
Final R indices ($I > 2\sigma(I)$) [a]	$R = 0.0273$, $R_w = 0.0334$
R indices (all data) [a]	$R = 0.0420$, $R_w = 0.1448$
Largest difference peak and hole (e Å^{-3})	1.30 and −1.96

[a] $R = \Sigma||F_o| - |F_c||/\Sigma|F_o|$. $R_w = [\Sigma w(|F_o| - |F_c|)^2/\Sigma wF_o^2]^{1/2}$, $w = [\sigma^2(F_o) + 0.0004|F_o|^2]^{-1}$.

Table 2
Selected bond lengths (Å) and bond angles (°) for complex **9**

Bond lengths			
Au–P	2.2726(7)	P–C(111)	1.821(3)
P–C(121)	1.812(3)	P–C(131)	1.816(3)
Au–C(1)	2.006(3)	C(1)–C(2)	1.194(4)
C(2)–C(3)	1.440(4)	C(3)–C(4)	1.398(4)
C(4)–C(5)	1.381(4)	C(5)–C(6)	1.389(4)
C(6)–C(7)	1.386(4)	C(7)–C(8)	1.382(4)
C(3)–C(8)	1.391(4)	C(6)–C(9)	1.505(4)
C(9)–O(1)	1.408(4)	O(1)–C(10)	1.439(4)
C(10)–C(11)	1.500(6)	C(11)–C(12)	1.513(6)
C(12)–O(2)	1.450(4)	C(9)–O(2)	1.408(4)
Bond angles			
P–Au–C(1)	177.5(1)	Au–P–C(111)	113.1(1)
Au–P–C(121)	112.6(1)	Au–P–C(131)	114.0(1)
Au–C(l)–C(2)	170.9(3)	C(1)–C(2)–C(3)	174.5(3)
C(2)–C(3)–C(4)	121.7(3)	C(3)–C(4)–C(5)	121.2(3)
C(4)–C(5)–C(6)	120.6(3)	C(5)–C(6)–C(7)	118.6(3)
C(6)–C(7)–C(8)	120.8(3)	C(2)–C(3)–C(8)	120.7(3)
C(3)–C(8)–C(7)	121.2(3)	C(5)–C(6)–C(9)	122.5(3)
C(7)–C(6)–C(9)	118.9(3)	C(6)–C(9)–O(1)	109.8(2)
C(6)–C(9)–O(2)	108.0(3)	C(9)–O(1)–C(10)	110.1(3)
O(1)–C(9)–O(2)	111.2(3)	O(1)–C(10)–C(11)	109.7(3)
C(10)–C(11)–C(12)	110.0(3)	C(12)–O(2)–C(9)	110.0(3)

complex **15** has an anomalously low oxidation potential (in this regard, its very low energy UV–vis transition and lack of facile deprotonation to the corresponding alkynyl complex can also be regarded as nonconforming). Oxidation potentials vary on phenyl substituent variation as 4-H < 4-CH{OC(O)Me}$_2$ < 4-CHO < 4-NO$_2$, the increasingly stronger electron-withdrawing groups resulting in increasing difficulty in oxidation. Oxidation potentials vary on phenyl substituents location as 3-CHO < 4-CHO, the former out of conjugation, the latter in conjugation with the metal. These results are consistent with the arylalkynyl bridge providing an efficient conduit for electronic communication.

2.5. Quadratic hyperpolarizabilities

We have determined the molecular quadratic nonlinearities of **1**–**12** and **15**, together with acetylenes utilized in the present study, using hyper-Rayleigh scattering at 1064 nm; the results of these studies, β_{exp}, are given in Table 4, together with the two-level-corrected values β_0, and corresponding data for relevant complexes. We have discussed earlier the potential inadequacies of the two-state model [13]. The low-energy band for these complexes is MLCT in character; higher-energy bands involve transitions with other ligands, which result in little change in dipole moment between ground and excited states, and hence little contribution to nonlinearity, so it is probable that the two-level-corrected values have some significance as an indicator of zero-frequency nonlinearity.

The tabulated data reveal that phenyl substituent variation results in β values increasing as 4-H < 4-CH{OC(O)Me}$_2$, 4-$\overline{CHO(CH_2)_3O}$ < 4-CHO < 4-NO$_2$, the expected trend for increasing acceptor strength in these dipolar molecules. In most instances, nonlinearities increase significantly on proceeding from precursor acetylene to product vinylidene or acetylide complex. Nonlinearities for gold complexes are significantly less than those for their ruthenium analogues, a result we have noted previously for related pairs of complexes [22]. Replacing PPh_3 by PMe_3 in proceeding from **9** to **10** results in a threefold increase in β_{exp} and β_0, the opposite result to that seen in an earlier study of 5-nitro-2-pyridylalkynyl complexes [15]; PMe_3 is a more basic phosphine, resulting in a more electron-rich gold donor, but PPh_3 provides for more extensive π-delocalization, and it is not immediately apparent which is the more important factor influencing the magnitude of β in these complexes. Phenyl substituent location affects β, in replacing 3-CHO by 4-CHO (proceeding from **12** to *trans*-[Ru(4-C≡CC_6H_4CHO)Cl(dppm)$_2$]), with the magnitude increasing upon formal conjugation of the metal center with the acceptor formyl unit; however, this result does not translate to increased corrected nonlinearities, experimentally indistinguishable β_0 values being observed. Vinylidene and acetylide complex pairs (**7**, **8** and **11**, **12**) have very similar nonlinearities.

2.6. Cubic hyperpolarizabilities

Third-order nonlinearities for **1**–**9**, **11**, **12** and **15** were determined by *Z*-scan at 800 nm, data being tabulated in Table 5. An electronic origin for cubic nonlinearities in related metal acetylide complexes has been demonstrated earlier by degenerate four-wave mixing measurements, and nonlinearities for the present series of compounds are therefore likely to be electronic in origin [5].

Nonlinearities for the new compounds are low, with large error margins in many instances, rendering the extraction of structure–property relationships difficult. Nevertheless, several points may be noted. Introduction of ligated gold in proceeding from **2** to **9** and replacing PMe_3 by PPh_3 in proceeding from **6** to **5** both result in increased γ_{real} and $|\gamma|$, and the γ_{real} and $|\gamma|$ values for **15** are larger than those of the 3- and 4-formylphenylvinylidene complex analogues.

3. Conclusions

The present studies have afforded complexes containing protected and exposed formylphenylalkynyl or -vinylidene ligands. As the aldehyde functional group can be derivatized in a variety of useful ways, complexes bearing these ligands should have utility in the assembly of extended structures. The electronic properties of these ligands are as predicted, their electron-withdrawing character being less than the strong nitro acceptor, and diminishing as the CHO substituent moves from *para* to *meta* position with respect to the alkynyl/vinylidene group. The magnitude of quadratic nonlinearities in these complexes largely parallels the effectiveness of this electron-withdrawing group. Cubic nonlinearities are in most cases too low to comment confidently, but the enhancement in γ_{real} on replacing PMe_3 by PPh_3 (proceeding from **6** to **5**) and replacing 4- and 3-formylvinylidene ligand by 2-formylvinylidene ligand

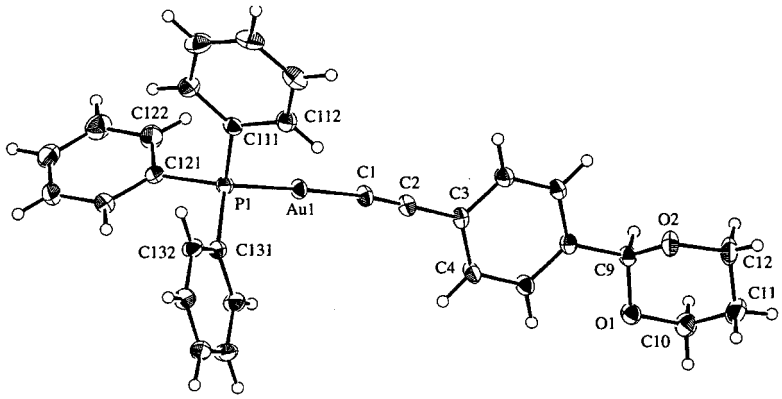

Fig. 1. Molecular geometry and atomic labeling scheme for [Au{C≡CC$_6$H$_4$CHO(CH$_2$)$_3$O}(PPh$_3$)] (**9**).

Table 3
Cyclic voltammetric data for ruthenium complexes [a]

Complex	$E_{1/2}$ $Ru^{II/III}$ (V)	$[i_{pc}/i_{pa}]$	Reference
[Ru(C≡CPh)(PPh$_3$)$_2$(η-C$_5$H$_5$)]	0.55	0.7	[6]
[Ru(4-C≡CC$_6$H$_4$CH{OC(O)Me}$_2$)(PPh$_3$)$_2$(η-C$_5$H$_5$)] (**3**)	0.59	1	This work
[Ru(4-C≡CC$_6$H$_4$CHO)(PPh$_3$)$_2$(η-C$_5$H$_5$)] (**4**)	0.67	0.9	This work
[Ru(4-C≡CC$_6$H$_4$NO$_2$)(PPh$_3$)$_2$(η-C$_5$H$_5$)]	0.73	1	[6]
trans-[Ru(C=CHPh)Cl(dppm)$_2$]PF$_6$	1.38	[b]	[1]
trans-[Ru(C≡CPh)Cl(dppm)$_2$]	0.55	1	[1]
trans-[Ru{4-C=CHC$_6$H$_4$CHO(CH$_2$)$_3$O}Cl(dppm)$_2$]PF$_6$ (**7**)	1.48	[b]	This work
trans-[Ru{4-C≡CC$_6$H$_4$CHO(CH$_2$)$_3$O}Cl(dppm)$_2$] (**8**)	0.51	1	This work
trans-[Ru(4-C=CHC$_6$H$_4$CHO)Cl(dppm)$_2$]PF$_6$	1.50	[b]	[1]
trans-[Ru(4-C≡CC$_6$H$_4$CHO)Cl(dppm)$_2$]	0.66	1	[1]
trans-[Ru(3-C=CHC$_6$H$_4$CHO)Cl(dppm)$_2$]PF$_6$ (**11**)	1.34	[b]	This work
trans-[Ru(3-C≡CC$_6$H$_4$CHO)Cl(dppm)$_2$] (**12**)	0.60	0.9	This work
trans-[Ru(2-C=CHC$_6$H$_4$CHO)Cl(dppm)$_2$]PF$_6$ (**15**)	1.23	[b]	This work

[a] Ferrocene/ferrocenium couple (0.56 V) as an internal standard.
[b] Nonreversible process.

Table 4
Experimental linear optical spectroscopic and quadratic NLO response parameters [a]

Compound	λ_{max} (nm) [ε, 10^4 M^{-1} cm^{-1}]	β_{exp} (10^{-30} esu) [b]	β_0 (10^{-30} esu) [c]	Reference
4-HC≡CC_6H_4CHO	271 [2.5]	7	4	This work
4-HC≡$CC_6H_4CH\{OC(O)Me\}_2$ (**1**)	252 [2.3]	11	7	This work
4-HC≡$CC_6H_4\overline{CHO\{CH_2\}_3O}$ (**2**)	250 [1.9]	27	20	This work
3-HC≡CC_6H_4CHO	332 [0.1]	21	12	This work
[Ru(C≡CPh)$(PPh_3)_2(\eta$-$C_5H_5)$]	310 [2.0]	16	10	[13]
[Ru(4-C≡$CC_6H_4CH\{OC(O)Me\}_2)(PPh_3)_2(\eta$-$C_5H_5)$] (**3**)	326 [2.3]	68	38	This work
[Ru(4-C≡$CC_6H_4CHO)(PPh_3)_2(\eta$-$C_5H_5)$] (**4**)	400 [2.3]	120	45	This work
[Ru(4-C≡$CC_6H_4NO_2)(PPh_3)_2(\eta$-$C_5H_5)$]	460 [8.5]	468	96	[7]
[Au(4-C≡$CC_6H_4CHO)(PPh_3)$] (**5**)	322 [5.0]	14	8	This work
[Au(4-C≡$CC_6H_4CHO)(PMe_3)$] (**6**)	322 [5.0]	[d]	–	This work
trans-[Ru{4-C=$CHC_6H_4\overline{CHO(CH_2)_3O}$}$Cl(dppm)_2$]$PF_6$ (**7**)	317 [1.3]	64	38	This work
trans-[Ru{4-C≡$CC_6H_4\overline{CHO(CH_2)_3O}$}$Cl(dppm)_2$] (**8**)	320 [1.2]	61	35	This work
[Au(4-C≡$CC_6H_4CHO\{CH_2\}_3O)(PPh_3)$] (**9**)	296 [1.7]	15	4	This work
[Au(4-C≡$CC_6H_4CHO\{CH_2\}_3O)(PMe_3)$] (**10**)	292 [0.8]	48	13	This work
trans-[Ru(3-C=$CHC_6H_4CHO)Cl(dppm)_2$]PF_6 (**11**)	320 [1.1]	45	26	This work
trans-[Ru(3-C≡$CC_6H_4CHO)Cl(dppm)_2$] (**12**)	321 [0.9]	58	34	This work
trans-[Ru(4-C≡$CC_6H_4CHO)Cl(dppm)_2$]	405 [6.0]	106	38	[1]
[Au(3-C≡$CC_6H_4CHO)(PPh_3)$] (**13**)	318 [0.5]	[d]	–	This work
[Au(3-C≡$CC_6H_4CHO)(PMe_3)$] (**14**)	322 [0.1]	[d]	–	This work
trans-[Ru(2-C=$CHC_6H_4CHO)Cl(dppm)_2$]PF_6 (**15**)	555 [0.2]	27	2	This work

[a] All measurements in thf solvent. All complexes are optically transparent at 1064 nm.
[b] HRS at 1064 nm; values $\pm 10\%$.
[c] HRS at 1064 nm corrected for resonance enhancement at 532 nm using the two-level model with $\beta_o = \beta[1-(2\lambda_{max}/1064)^2][1-(\lambda_{max}/1064)^2]$; damping factors not included.
[d] Too low to measure.

Table 5
Experimental linear optical spectroscopic and cubic NLO response parameters [a]

Compound	λ_{max} (nm) [ε, 10^4 M^{-1} cm^{-1}]	γ_{real} (10^{-36} esu) [b]	γ_{imag} (10^{-36} esu) [b]	$\lvert\gamma\rvert$ (10^{-36} esu) [b]	Reference
4-HC≡CC_6H_4CHO	271 [2.5]	17 ± 8	0	17 ± 8	This work
4-HC≡$CC_6H_4CH\{OC(O)Me\}_2$ (**1**)	252 [2.3]	-180 ± 80	5 ± 5	180 ± 80	This work
[Ru(4-C≡$CC_6H_4CH\{OC(O)Me\}_2)(PPh_3)_2(\eta$-$C_5H_5)$] (**3**)	326 [2.4]	100 ± 100	0	100 ± 100	This work
[Ru(4-C≡$CC_6H_4CHO)(PPh_3)_2(\eta$-$C_5H_5)$] (**4**)	400 [2.3]	-75 ± 50	210 ± 50	220 ± 60	This work
[Au(4-C≡$CC_6H_4CHO)(PPh_3)$] (**5**)	322 [5.0]	300 ± 150	0	300 ± 150	This work
[Au(4-C≡$CC_6H_4CHO)(PMe_3)$] (**6**)	322 [5.0]	35 ± 20	45 ± 30	60 ± 35	This work
4-HC≡$CC_6H_4\overline{CHO(CH_2)_3O}$ (**2**)	250 [1.9]	15 ± 7	3 ± 3	15 ± 7	This work
trans-[Ru{4-C=$CHC_6H_4\overline{CHO(CH_2)_3O}$}$Cl(dppm)_2$]$PF_6$ (**7**)	317 [1.3]	75 ± 75	0	75 ± 75	This work
trans-[Ru{4-C≡$CC_6H_4\overline{CHO(CH_2)_3O}$}$Cl(dppm)_2$] (**8**)	320 [1.2]	50 ± 50	0	50 ± 50	This work
[Au(4-C≡$CC_6H_4\overline{CHO(CH_2)_3O}$}$(PPh_3)$] (**9**)	296 [1.7]	210 ± 100	0	210 ± 100	This work
[Au{4-C≡$CC_6H_4\overline{CHO(CH_2)_3O}$}$(PMe_3)$] (**10**)	292 [0.8]	[c]	[c]		This work
trans-[Ru(3-C=$CHC_6H_4CHO)Cl(dppm)_2$]PF_6 (**11**)	320 [1.1]	200 ± 200	0	200 ± 200	This work
trans-[Ru(3-C≡$CC_6H_4CHO)Cl(dppm)_2$] (**12**)	321 [0.9]	150 ± 150	0	150 ± 150	This work
[Au(3-C≡$CC_6H_4CHO)(PPh_3)$] (**13**)	318 [0.5]	[d]	[d]		This work
[Au(3-C≡$CC_6H_4CHO)(PMe_3)$] (**14**)	322 [0.1]	[d]	[d]		This work
trans-[Ru(2-C=$CHC_6H_4CHO)Cl(dppm)_2$]PF_6 (**15**)	555 [0.2]	450 ± 150	150 ± 60	470 ± 160	This work
trans-[Ru(4-C=$CHC_6H_4CHO)Cl(dppm)_2$]PF_6	403 [1.9]	0	<20	<20	[1]

[a] All measurements as THF solutions (all complexes are optically transparent at 800 nm).
[b] All results are referenced to silica, nonlinear refractive index $n_2 = 3 \times 10^{-16}$ cm^2 W^{-1}.
[c] Too low to measure.
[d] Sample scattered light.

(proceeding to **15**) contrast with the effect of these structural modifications on β values.

4. Experimental

4.1. General conditions, reagents and instruments

All reactions were performed under a nitrogen atmosphere with the use of standard Schlenk techniques unless otherwise stated. Dichloromethane and Et_3N were dried by distilling over CaH_2, Et_2O and THF were dried by distilling over sodium–benzophenone, and other solvents were used as received. 'Petroleum spirit' refers to a fraction of petroleum ether of boiling range 60–80 °C. Chromatography was carried out on silica gel (230–400 mesh ASTM) or basic ungraded alumina.

The following reagents were prepared by the literature procedures: *cis*-$[RuCl_2(dppm)_2]$ [23], $[AuCl(PPh_3)]$ [24], $[AuCl(PMe_3)$ [25], 4-$HC{\equiv}CC_6H_4CHO$ [26], 3-$HC{\equiv}CC_6H_4CHO$ [26], 2-$HC{\equiv}CC_6H_4CHO$ [26]. Ammonium hexafluorophosphate (Aldrich), 4-$MeC_6H_4SO_3H{\cdot}H_2O$ (Aldrich), 1,3-propanediol (Aldrich), $FeCl_3$ (Ajax) and acetic anhydride (Aldrich) were used as received.

EI (electron impact) mass spectra (both unit resolution and high resolution (HR)) were recorded using a VG Autospec instrument (70 eV electron energy, 8 kV accelerating potential) and secondary ion mass spectra (SIMS) were recorded using a VG ZAB 2SEQ instrument (30 kV Cs^+ ions, current 1 mA, accelerating potential 8 kV, 3-nitrobenzyl alcohol matrix) at the Research School of Chemistry, Australian National University; peaks are reported as m/z (assignment, relative intensity). Microanalyses were carried out at the Research School of Chemistry, Australian National University. IR spectra were recorded either as 1% KBr discs or CH_2Cl_2 solutions using a Perkin–Elmer System 2000 FTIR. ^{1}H-, ^{31}P-, and ^{13}C-NMR spectra were recorded using a Varian Gemini-300 FT NMR spectrometer and are referenced to residual $CHCl_3$ (7.24 ppm), $CHCl_3$-*d* (77.0 ppm) or external 85% H_3PO_4 (0.0 ppm), respectively. The assignments follow the numbering scheme shown in Fig. 2. UV–vis spectra of solutions were recorded in THF in 1 cm quartz cells using a Cary 4 spectrophotometer. Electrochemical measurements were recorded using a MacLab 400 interface and MacLab potentiostat from ADInstruments. The supporting electrolyte was 0.1 M $[N^nBu_4][PF_6]$ in distilled, deoxygenated CH_2Cl_2. Solutions containing ca. 1×10^{-3} M complex were maintained under nitrogen. Measurements were carried out at 25 °C using platinum disc working-, Pt wire auxillary- and Ag/AgCl reference-electrodes, such that the ferrocene/ferrocenium redox couple was located at 0.56 V with a peak separation of around 0.09 V. Scan rates were typically 100 mV s^{-1}.

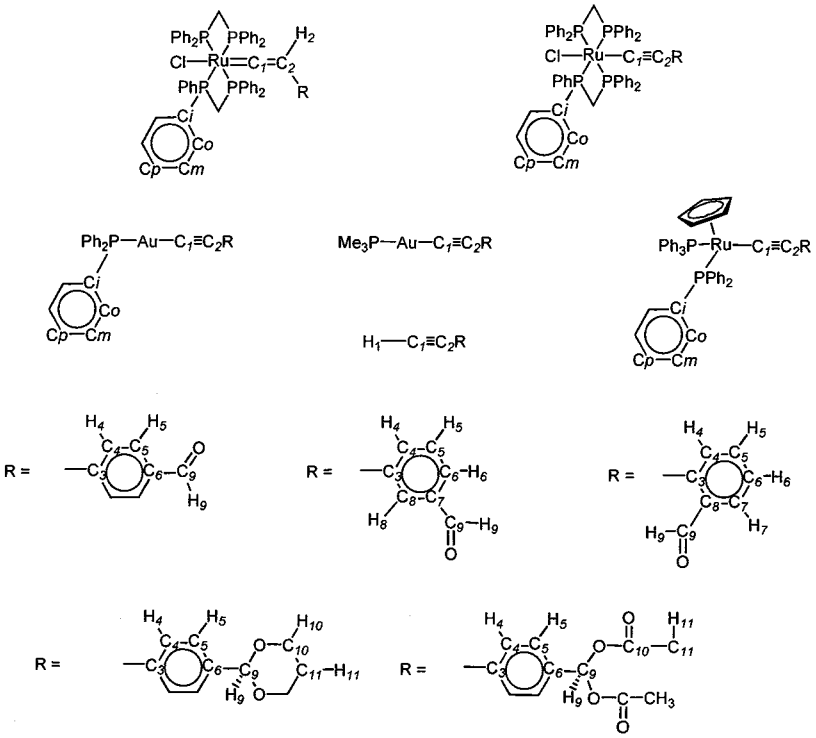

Fig. 2. Numbering scheme for NMR spectral assignments for **1**–**15**.

4.2. Synthesis of terminal acetylenes

4.2.1. 4-HC≡CC$_6$H$_4$CH{OC(O)Me}$_2$ (1)

4-HC≡CC$_6$H$_4$CHO (1.00 g, 7.69 mmol) was stirred in Ac_2O (6 ml) for 15 min, and then 0.1 g of anhydrous ferric chloride was added. After stirring for a further 20 min, the reaction mixture was poured into 50 ml of hexane and 10 ml of water. The aqueous phase was washed with 3 × 30 ml portions hexane, and the combined organic extracts were washed with 3 × 30 ml water. The organic phase was dried and concentrated to give the white product (690 mg, 39%). Anal. Found: C, 66.45; H, 5.31. Calc. for $C_{13}H_{12}O_4$: C, 67.23; H, 5.21%. IR (CH_2Cl_2, cm^{-1}): ν(HC≡) 3297, ν(C≡C) 2111. UV–vis: λ (nm) (ε, M^{-1} cm^{-1}) (THF): 252 (17 000). ^{1}H-NMR: ($CDCl_3$, 300 MHz): $\delta = 2.11$ (s, 6H, H_{11}), 3.10 (s, 1H, H_1), 7.45 (d, $J_{HH} = 9$ Hz, 2H, H_4), 7.51 (d, $J_{HH} = 9$ Hz, 2H, H_5), 7.64 (s, 1H, H_9). SIMS: 232 ([M]$^+$, 20), 189 ([M − C(O)Me]$^+$, 25), 173 ([M − OC(O)Me]$^+$, 20), 129 ([M − MeC(O)OC(O)Me − H]$^+$, 100), 101 ([M − CH{OC(O)Me}$_2$]$^+$, 40). HRMS; m/z: Found: 232.0735. Calc. for $C_{13}H_{12}O_4$: 232.0737.

4.2.2. 4-HC≡CC$_6$H$_4$CHO(CH$_2$)$_3$O (2)

4-HC≡CC$_6$H$_4$CHO (200 mg, 1.54 mmol), 4-MeC$_6$H$_4$SO$_3$H·H$_2$O (40 mg, 0.21 mmol) and HO(CH$_2$)$_3$OH (140 mg, 1.85 mmol) were stirred in CH_2Cl_2 (25 ml) for 8 h. The solution was neutralized with saturated $NaHCO_3$ solution, washed with water and dried with $MgSO_4$. The solvent was removed under reduced pressure to obtain the pale-brown product (204 mg, 69%). Anal. Found: C, 75.89; H, 5.93. Calc. for $C_{12}H_{12}O_2$: C, 76.57; H, 6.43%. IR (CH_2Cl_2, cm^{-1}): ν(C≡C) 2112. UV–vis: λ (nm) (ε, M^{-1} cm^{-1}) (THF): 250 (18 900). ^{1}H-NMR: ($CDCl_3$, 300 MHz): $\delta = 1.44$ (m, 1H, H_{11}), 2.10–2.30 (m, 1H, H_{11}), 3.05 (s, 1H, H_1), 3.90–4.05 (m, 2H, H_{10}), 4.20–4.30 (m, 2H, H_{10}), 5.47 (s, 1H, H_9), 7.42 (d, $J_{HH} = 9$ Hz, 2H, H_4), 7.48 (d, $J_{HH} = 9$ Hz, 2H, H_5). EIMS: 188 ([M]$^+$, 100), 129 ([M − H − (CH$_2$)$_3$O]$^+$, 95). HRMS; m/z: Found: 188.0836. Calc. for $C_{12}H_{12}O_2$: 188.0837.

4.3. Synthesis of metal complexes

4.3.1. [Ru(4-C≡CC$_6$H$_4$CH{OC(O)Me}$_2$)(PPh$_3$)$_2$(η-C$_5$H$_5$)] (3)

[RuCl(PPh$_3$)$_2$(η-C$_5$H$_5$)] (300 mg, 0.41 mmol), NH_4PF_6 (101 mg, 0.62 mmol) and 4-HC≡CC$_6$H$_4$CH{OC(O)Me}$_2$ (**1**) (115 mg, 0.50 mmol) were added to MeOH (25 ml), and the resultant mixture was refluxed with stirring for 1 h, and then allowed to cool. A solution of CH_3ONa in MeOH (1 M, 5 ml) was added, the mixture was stirred for 5 min, and then the solvent removed under reduced pressure. Column chromatography with 1:1 petroleum spirit–CH_2Cl_2 yielded the orange product (235 mg, 62%). Anal. Found: C, 70.19; H, 5.40%. Calc. for $C_{54}H_{46}O_4P_2Ru$: C, 70.35; H, 5.03%. IR (CH_2Cl_2, cm^{-1}): ν(C≡C) 2066. UV–vis: λ (nm) (ε, M^{-1} cm^{-1}) (THF): 327 (22 600). ^{1}H-NMR ($CDCl_3$, 300 MHz): $\delta = 2.10$ (m, 6H, Me), 4.29 (s, 5H, C_5H_5), 7.10–7.50 (m, 30H, Ph), 7.64 (s, 1H, H_9). ^{31}P-NMR ($CDCl_3$, 121 MHz): $\delta = 51.3$. SIMS: 922 ([M]$^+$, 40), 863 ([M − OC(O)Me]$^+$, 5), 660 ([M − PPh$_3$]$^+$, 10), 429 ([M − PPh$_3$ − C≡CC$_6$H$_4$CH{OC(O)Me}$_2$]$^+$, 100).

4.3.2. [Ru(4-C≡CC$_6$H$_4$CHO)(PPh$_3$)$_2$(η-C$_5$H$_5$)] (4)

[Ru(4-C≡CC$_6$H$_4$CH{OC(O)Me}$_2$)(PPh$_3$)$_2$(η-C$_5$H$_5$)] (**3**) (300 mg, 0.33 mmol) was dissolved in MeOH (15 ml) and a solution of CH_3ONa in MeOH (1 M, 5 ml) was added. The mixture was stirred at room temperature (r.t.) for 2 h and then the solvent reduced, yielding the orange–red product (221 mg, 73%). Anal. Found: C, 72.32; H, 5.32. Calc. for $C_{50}H_{40}OP_2Ru$: C, 73.25; H, 4.92%. IR (CH_2Cl_2, cm^{-1}): ν(C≡C) 2053. UV–vis: λ (nm) (ε, M^{-1} cm^{-1}) (THF): 400 (23 000). ^{1}H-NMR ($CDCl_3$, 300 MHz,): $\delta = 4.33$ (s, 5H, C_5H_5), 6.90–7.60 (m, 34H, Ph), 9.85 (s, 1H, H_9). ^{31}P-NMR ($CDCl_3$, 121 MHz): $\delta = 51.0$. SIMS: 820 ([M]$^+$, 100), 691 ([M − C≡CC$_6$H$_4$CHO]$^+$, 25), 558 ([M − PPh$_3$ − H]$^+$, 20), 429 ([Ru(PPh$_3$)(η-C$_5$H$_5$)]$^+$, 45).

4.3.3. [Au(4-C≡CC$_6$H$_4$CHO)(PPh$_3$)] (5)

[AuCl(PPh$_3$)] (200 mg, 0.40 mmol) and 4-HC≡CC$_6$H$_4$CHO (57 mg, 0.44 mmol) were stirred in a solution of CH_3ONa in MeOH (0.1 M, 15 ml) for 16 h. A solid precipitate was filtered to yield the yellow product (135 mg, 57%). Anal. Found: C, 54.62; H, 3.39. Calc. for $C_{27}H_{20}AuOP$: C, 55.12; H, 3.43%. IR (CH_2Cl_2, cm^{-1}): ν(C≡C) 2115. UV–vis: λ (nm) (ε, M^{-1} cm^{-1}) (THF): 322 (50 000). ^{1}H-NMR ($CDCl_3$, 300 MHz): $\delta = 7.30$–7.80 (m, 19H, Ph), 9.94 (s, 1H, H_9). ^{31}P-NMR ($CDCl_3$, 121 MHz): $\delta = 42.8$. SIMS: 1047 ([M + Au(PPh$_3$)]$^+$, 75), 721 ([Au(PPh$_3$)$_2$]$^+$, 20), 589 ([M]$^+$, 30), 459 ([Au(PPh$_3$)]$^+$, 100).

4.3.4. [Au(4-C≡CC$_6$H$_4$CHO)(PMe$_3$)] (6)

[AuCl(PMe$_3$)] (154 mg, 0.50 mmol) and 4-HC≡CC$_6$H$_4$CHO (72 mg, 0.55 mmol) were stirred in a solution of CH_3ONa in MeOH (0.1 M, 15 ml) for 16 h. The solid precipitate was collected by filtration to yield the pale-yellow product (156 mg, 78%). Anal. Found: C, 36.87; H, 3.71. Calc. for $C_{12}H_{14}AuOP$: C, 35.84; H, 3.51%. IR (CH_2Cl_2, cm^{-1}): ν(C≡C) 2112. UV–vis: λ (nm) (ε, M^{-1} cm^{-1}) (THF): 322 (49 800). ^{1}H-NMR ($CDCl_3$, 300 MHz): $\delta = 1.51$ (d, $J_{HP} = 10$ Hz, 9H, Me), 7.54 (d, $J_{HH} = 8$ Hz, 2H, C_6H_4), 7.72 (d, $J_{HH} = 8$ Hz, 2H, C_6H_4), 9.92 (s, H_9). ^{31}P-NMR ($CDCl_3$, 121 MHz): $\delta = 1.6$. SIMS: 675 ([M + Au(PMe$_3$) − 2H]$^+$, 40), 403 ([M]$^+$, 60), 349 ([Au(PMe$_3$)$_2$]$^+$, 45), 273 ([Au(PMe$_3$)]$^+$, 80).

*4.3.5. trans-[Ru(4-C=CHC$_6$H$_4$CHO(CH$_2$)$_3$O)-Cl(dppm)$_2$][PF$_6$] (**7**)*

cis-[RuCl$_2$(dppm)$_2$] (200 mg, 0.21 mmol), NH_4PF_6 (70 mg, 0.43 mmol) and **2** (48 mg, 0.26 mmol) were added to CH_2Cl_2 (25 ml), and the resultant mixture stirred for 4 h. Petroleum spirit (50 ml) was added, and the solvent removed under vacuum. The solid material was triturated with ether and then filtered to yield the pale-red product (220 mg, 84%). Anal. Found: C, 59.99; H, 4.78. Calc. for $C_{62}H_{56}ClF_6O_2P_5Ru$: C, 60.13; H, 4.56%. IR (KBr, cm^{-1}): ν(PF) 839. UV–vis: λ (nm) (ε, $M^{-1}\,cm^{-1}$) (THF): 317 (ε 13 400). ^{1}H-NMR ($CDCl_3$, 300 MHz): $\delta = 1.40$ (m, 1H, H_{11}), 2.10–2.20 (m, 1H, H_{11}), 2.95 (m, 1H, H_2), 3.85–4.25 (m, 4H, H_{10}), 5.06 (m, 2H, PCH_2P), 5.30 (m, 2H, PCH_2P), 5.35 (s, 1H, H_9), 5.48 (d, $J_{HH} = 8$ Hz, 2H, H_4), 6.85 (d, $J_{HH} = 8$ Hz, 2H, H_5), 7.10–7.50 (m, 40H, Ph). ^{31}P-NMR ($CDCl_3$, 121 MHz): $\delta = -15.5$. SIMS: 1092 ($[M - PF_6]^+$, 15), 905 $[RuCl(dppm)_2]^+$, 90), 869 ($[Ru(dppm)_2 - H]^+$, 100), 485 ($[Ru(dppm)]^+ - H$, 90).

*4.3.6. trans-[Ru{4-C≡CC$_6$H$_4$CHO(CH$_2$)$_3$O}-Cl(dppm)$_2$]·0.5CH$_2$Cl$_2$ (**8**)*

trans-[Ru{4-C=CHC$_6$H$_4$CHO(CH$_2$)$_3$O}Cl(dppm)$_2$]-[PF_6] (**7**) (200 mg, 0.16 mmol) was added to CH_2Cl_2 (25 ml) and Et_3N (1 ml) and the resultant mixture stirred for 10 min at r.t. The mixture was passed through an alumina plug, petroleum spirit (50 ml) was added, and the resulting precipitate was collected and washed with petroleum spirit yielding the pale-red product (153 mg, 87%). Anal. Found: C, 66.85; H, 5.09. Calc. for $C_{62.5}H_{56}Cl_2O_2P_4Ru$: C, 66.14; H, 4.97%. IR (CH_2Cl_2, cm^{-1}): ν(C≡C) 2081. UV–vis: λ (nm) (ε, $M^{-1}\,cm^{-1}$) (THF): 320 (11 600). ^{1}H-NMR ($CDCl_3$, 300 MHz): $\delta = 1.40$ (m, 1H, H_{11}), 2.20–2.40 (m, 1H, H_{11}), 3.80–4.00 (m, 2H, H_{10}), 4.20–4.30 (m, 2H, H_{10}), 4.88 (m, 4H, PCH_2P), 5.27 (s, 1H, CH_2Cl_2), 5.35 (s, H_9), 5.97 (d, $J_{HH} = 8$ Hz, 2H, H_4), 6.90–7.50 (m, 42H, Ph + H_5). ^{31}P-NMR ($CDCl_3$, 121 MHz): $\delta = -6.1$. SIMS: 1092 ($[M]^+$, 100), 905 ($[RuCl(dppm)_2]^+$, 15), 869 ($[Ru(dppm)_2 - H]^+$, 50), 486 ($[Ru(dppm)]^+$, 30).

*4.3.7. [Au{4-C≡CC$_6$H$_4$CHO(CH$_2$)$_3$O}(PPh$_3$)] (**9**)*

[AuCl(PPh_3)] (100 mg, 0.20 mmol) and **2** (46 mg, 0.24 mmol) were stirred in a solution of CH_3ONa in MeOH (0.1 M, 15 ml) for 16 h. A solid precipitate was collected by filtration to yield the pale-yellow product (121 mg, 93%). Anal. Found: C, 54.66; H, 4.32. Calc. for $C_{30}H_{26}AuO_2P$: C, 54.88; H, 4.46%. IR (CH_2Cl_2, cm^{-1}): ν(C≡C) 2117. UV–vis: λ (nm) (ε, $M^{-1}\,cm^{-1}$) (THF): 296 (16 600), 288 (30 600). ^{1}H-NMR ($CDCl_3$, 300 MHz): $\delta = 1.43$ (m, 1H, H_{11}), 2.10–2.30 (m, 1H, H_{11}), 3.90–4.00 (m, 2H, H_{10}), 4.20–4.30 (m, 2H, H_{10}), 5.45 (s, 1H, H_9), 7.35 (d, $J_{HH} = 8$ Hz, 2H, H_4), 7.38–7.60 (m, 17H, Ph + H_5). ^{31}P-NMR ($CDCl_3$, 121 MHz): 42.8. SIMS: 721 ($[Au(PPh_3)_2]^+$, 20), 647 ($[M]^+$, 30), 459 ($[Au(PPh_3)]^+$, 100).

*4.3.8. [Au{4-C≡CC$_6$H$_4$CHO(CH$_2$)$_3$O}(PMe$_3$)]·1CH$_3$CH$_2$OH (**10**)*

[AuCl(PMe_3)] (100 mg, 0.324 mmol) and **2** (80 mg, 0.40 mmol) were stirred in a solution of CH_3ONa in MeOH (0.1 M, 15 ml) for 16 h. A solid precipitate was collected by filtration to yield the pale-yellow product (108 mg, 72%). Anal. Found: C, 40.43; H, 4.28. Calc. for $C_{17}H_{26}AuO_3P$: C, 40.33; H, 5.18%. IR (CH_2Cl_2, cm^{-1}): ν(C≡C) 2118. UV–vis: λ (nm) (ε, $M^{-1}\,cm^{-1}$) (THF): 292 (7600), 285 (23 200). ^{1}H-NMR ($CDCl_3$, 300 MHz): $\delta = 1.20$ (t, $J_{HH} = 4$ Hz, 3H, CH_3), 1.42 (br s, lH, H_{11}), 1.52 (br s, 9H, Me), 2.10–2.30 (m, lH, H_{11}), 3.67 (q, $J_{HH} = 6$ Hz, 2H, CH_2), 3.80–4.00 (m, 2H, H_{10}), 4.15–4.30 (m, 2H, H_{10}), 5.44 (s, 1H, H_9), 7.33 (d, $J_{HH} = 8$ Hz, 2H, H_4), 7.44 (d, $J_{HH} = 8$ Hz, 2H, H_5). ^{31}P-NMR ($CDCl_3$, 121 MHz): $\delta = 1.7$. SIMS: 459 ($[M + Au(PMe_3)]^+$, 10), 459 ($[M - H]^+$, 100).

*4.3.9. trans-[Ru(3-C=CHC$_6$H$_4$CHO)Cl(dppm)$_2$][PF$_6$] (**11**)*

cis-[RuCl$_2$(dppm)$_2$] (400 mg, 0.43 mmol), NH_4PF_6 (140 mg, 0.86 mmol) and 3-HC≡CC$_6$H$_4$CHO (174 mg, 0.86 mmol) were added to CH_2Cl_2 (25 ml), and the resultant mixture refluxed for 2 h. Petroleum spirit (50 ml) was added, and the resulting precipitate was collected and washed with ether to afford the pale-red solid (409 mg, 76%). Anal. Found: C, 59.67; H, 4.44. Calc. for $C_{59}H_{50}ClF_6OP_5Ru$: C, 60.03; H, 4.27%. IR (KBr, cm^{-1}): ν(PF) 839. UV–vis: λ (nm) (ε, $M^{-1}\,cm^{-1}$) (THF): 320 (10 900). ^{1}H-NMR ($CDCl_3$, 300 MHz): $\delta = 3.13$ (m, 1H, H_2), 5.12 (m, 2H, PCH_2P), 5.32 (m, 2H, PCH_2P), 5.75–6.90 (4H, H_4, H_5), 7.10–7.60 (m, 40H, Ph), 9.54 (s, H_9). ^{31}P-NMR ($CDCl_3$, 121 MHz): $\delta = -15.9$. SIMS: 1035 ($[M - PF_6]^+$, 40), 999 ($[M - Cl - PF_6]^+$, 10), 904 ($[RuCl(dppm)_2]^+$, 70), 869 ($[Ru(dppm) - H]^+$, 100).

*4.3.10. trans-[Ru(3-C≡CC$_6$H$_4$CHO)Cl(dppm)$_2$] (**12**)*

cis-[RuCl$_2$(dppm)$_2$] (300 mg, 0.32 mmol), NH_4PF_6 (104 mg, 0.64 mmol) and 3-HC≡CC$_6$H$_4$CHO (90 mg, 0.69 mmol) were added to CH_2Cl_2 (25 ml), and the resultant mixture stirred for 4 h. Triethylamine (1 ml) and petroleum spirit (20 ml) were then added, and the solution filtered through an alumina plug. The solvent was removed under vacuum, the solid was then triturated with petroleum spirit and filtered to afford the yellow product (156 mg, 83%). Anal. Found: C, 68.06; H, 4.75%. Calc. for $C_{59}H_{49}ClOP_4Ru$: C, 68.50; H, 4.77%. IR (CH_2Cl_2, cm^{-1}): ν(C≡C) 2075. UV–vis: λ (nm) (ε, $M^{-1}\,cm^{-1}$) (THF): 321 (9500), 260 (32 300). ^{1}H-NMR ($CDCl_3$, 300 MHz): $\delta = 4.89$ (m, 4H, PCH_2P), 6.28 (d, $J_{HH} = 8$ Hz, lH, H_4 or H_6), 6.39 (s, 1H, H_8), 7.05–7.60 (m, 42H, Ph + H_5 + H_4 or H_6), 9.54 (s, 1H, H_9). ^{31}P-NMR ($CDCl_3$, 121 MHz): $\delta = -6.0$. SIMS: 1034 ($[M - H]^+$, 100), 999 ($M - Cl]^+$, 20), 905

($[RuCl(dppm)_2]^+$, 25), 869 ($[Ru(dppm)_2 - H]^+$, 60), 485 ($[Ru(dppm) - H]^+$, 35).

4.3.11. [Au(3-C≡CC$_6$H$_4$CHO)(PPh$_3$)] (13)

[AuCl(PPh$_3$)] (200 mg, 0.404 mmol) and 3-HC≡CC$_6$H$_4$CHO (63 mg, 0.49 mmol) were stirred in a solution of CH_3ONa in MeOH (0.1 M, 15 ml) for 16 h. The solid precipitate was washed with petroleum ether and filtered to yield the pale-yellow product (136 mg, 57%). Anal. Found: C, 54.43; H, 3.53. Calc. for $C_{27}H_{20}AuOP$: C, 55.11; H, 3.43%. IR (CH_2Cl_2, cm^{-1}): ν(C≡C) 2120. UV–vis: λ (nm) (ε, $M^{-1}\,cm^{-1}$) (THF): 318 (4700), 286 (18 400). ^{1}H-NMR ($CDCl_3$, 300 MHz): $\delta = 7.30$–7.80 (m, 19H, Ph), 9.93 (s, 1H, H_9). ^{31}P-NMR ($CDCl_3$, 121 MHz): $\delta = 42.9$. SIMS; 721 ($[Au(PPh_3)_2]^+$, 50), 589 ($[M]^+$, 5), 459 ($[Au(PPh_3)]^+$, 100).

4.3.12. [Au(3-C≡CC$_6$H$_4$CHO)(PMe$_3$)]·2C$_6$H$_6$ (14)

[AuCl(PMe$_3$)] (200 mg, 0.65 mmol) and 3-HC≡CC$_6$H$_4$CHO (101 mg, 0.78 mmol) were stirred in a solution of CH_3ONa in MeOH (0.1 M, 15 ml) for 16 h. The solid precipitate was collected by filtration and washed with petroleum spirit to yield the off-white product which was recrystallized from benzene (167 mg, 64%). Anal. Found: C, 50.75; H, 3.95. Calc. for $C_{24}H_{38}AuOP$: C, 51.62; H, 4.69%. IR (CH_2Cl_2, cm^{-1}): ν(C≡C) 2116. UV–vis: λ (nm) (ε, $M^{-1}\,cm^{-1}$) (THF): 322 (1000). ^{1}H-NMR ($CDCl_3$, 300 MHz): $\delta = 1.54$ (br s, 9H, Me), 7.30–8.00 (m, 4H, C_6H_4), 7.32 (s, 12H, C_6H_6), 9.92 (s, 1H, H_9). ^{31}P-NMR ($CDCl_3$, 121 MHz): $\delta = 1.6$. SIMS; 675 ($[M + Au(PMe_3) - 2H]^+$, 15), 403 ($[M]^+$, 5), 349 ($[Au(PMe_3)_2]^+$, 100), 273 ($[Au(PMe_3)]^+$, 60).

4.3.13. trans-[Ru(2-C=CHC$_6$H$_4$CHO)Cl(dppm)$_2$][PF$_6$] (15)

cis-[$RuCl_2$(dppm)$_2$] (300 mg, 0.32 mmol), NH_4PF_6 (104 mg, 0.64 mmol) and 2-HC≡CC$_6$H$_4$CHO (90 mg, 0.69 mmol) were added to CH_2Cl_2 (25 ml), and the resultant mixture stirred for 4 h. The solution was filtered, petroleum spirit (20 ml) was added, and the solvent removed under vacuum. The solid was triturated with ether and the purple solid was collected by filtration (305 mg, 81%). Anal. Found: C, 59.95; H, 4.69. Calc. for $C_{59}H_{50}ClF_6OP_5Ru$: C, 60.03; H, 4.27%. IR (KBr, cm^{-1}): ν(PF) 841. UV–vis: λ (nm) (ε, $M^{-1}\,cm^{-1}$) (THF): 555 (2000), 355 (7400). ^{1}H-NMR ($CDCl_3$, 300 MHz): $\delta =$ 5.25 (m, 2H, PCH_2P), 5.39 (m, 2H, PCH_2P), 5.67 (d, $J_{HH} = 9$ Hz, 1H, H_7), 6.40 (m, 1H, H_2), 6.80–7.60 (m, 43H, Ph + C_6H_4), 8.53 (s, 1H, H_9). ^{31}P-NMR ($CDCI_3$, 121 MHz): $\delta = -7.6$. LDTOFMS; 1059 ($[M - PF_6 +$ Na$]^+$, 100), 869 ($[Ru(dppm)_2 - H]^+$, 35).

4.4. X-ray crystallographic study of 9

Crystals suitable for the X-ray structural analysis were grown by liquid diffusion of MeOH into a CH_2Cl_2 solution of **9** at r.t. A single pale-yellow prism was mounted on a fine glass capillary using Paratone oil, and data were collected at 200 K on a Nonius Kappa-CCD diffractometer using graphite-monochromated Mo–K_α radiation. The unit cell parameters were obtained by least-squares refinement [27] of 38310 reflections with $2.9 \leq \theta \leq 30.0$. The data were corrected for absorption using numerical methods [28], implemented from within maXus [29]; equivalent reflections were merged. The structure was solved by direct methods [30] and expanded using Fourier techniques [31]. Non-hydrogen atoms were refined anisotropically; hydrogen atoms were included in idealized positions which were frequently recalculated. The final cycle of full-matrix least-squares refinement on F was based on 5733 observed reflections ($I > 2\sigma(I)$) and 307 variable parameters, and converged to $R = 0.027$. Selected crystal data and structure refinement parameters are tabulated in Table 1.

4.5. Hyper–Rayleigh scattering measurements

An injection-seeded Nd:YAG laser (Q-switched Nd:YAG Quanta Ray GCR5, 1064 nm, 8 ns pulses, 10 Hz) was focused into a cylindrical cell (7 ml) containing the sample. The intensity of the incident beam was varied by the rotation of a half-wave plate placed between crossed polarizers. Part of the laser pulse was sampled by a photodiode to measure the vertically polarized incident light intensity. The frequency doubled light was collected by an efficient condenser system and detected by a photomultiplier. The harmonic and linear scatterings were distinguished by appropriate filters; gated integrators were used to obtain the intensities of the incident and harmonic scattered light. The absence of a luminescence contribution to the harmonic signal was confirmed by using interference filters at different wavelengths near 532 nm. All measurements were performed in THF using *p*-nitroaniline ($\beta = 21.4 \times 10^{-30}$ esu) [32] as a reference. The absorption of the scattered light was negligible as the solutions were sufficiently dilute. Further details on the experimental procedure have been reported in Refs. [33,34].

4.6. Z-scan measurements

Measurements were performed at 800 nm using a system consisting of a Coherent Mira Ar-pumped Ti-sapphire laser generating a mode-locked train of ca. 100 fs pulses and a home-built Ti-sapphire regenerative amplifier pumped with a frequency-doubled Q-switched pulsed YAG laser (Spectra Physics GCR) at 30 Hz and employing chirped pulse amplification. The solutions were examined in a glass cell with a 0.1 cm path length. The Z-scans were recorded at two concentrations for each compound and the real and imaginary parts of the nonlinear phase change were determined by numerical

fitting [35]. The real and imaginary parts of the hyperpolarizability of the solute were then calculated by assuming linear concentration dependencies of the solution susceptibility. The nonlinearities and light intensities were calibrated using measurements of a 1 mm thick silica plate for which the nonlinear refractive index $n_2 = 3 \times 10^{-16}$ cm^2 W^{-1} was assumed.

5. Supplementary material

Crystallographic data for structural analysis have been deposited with the Cambridge Crystallographic Data Centre, CCDC no. 160385 for **9**. Copies of this information may be obtained free of charge from The Director, CCDC, 12 Union Road, Cambridge, CB2 1EZ, UK (Fax: +44-1223-336033; e-mail: deposit@ccdc.cam.ac.uk or www: http://www.ccdc.cam.ac.uk).

Acknowledgements

We thank the Australian Research Council (M.G.H.), the Belgian Government (Grant No. IUAP-PIV/11) (A.P.), the Fund for Scientific Research-Flanders (G.0338.98, G.0407.98) (A.P.), the K.U. Leuven (GOA/2000/03) (A.P.) for supporting this work, and Johnson–Matthey Technology Centre (M.G.H.) for the generous loan of ruthenium salts. M.P.C. held an ARC Australian Postdoctoral Research Fellowship, N.T.L. was an Australian Postgraduate Awardee and M.G.H. holds an ARC Australian Senior Research Fellowship.

References

[1] S.K. Hurst, M.P. Cifuentes, J.P.L. Morrall, N.T. Lucas, I.R. Whittall, M.G. Humphrey, I. Asselberghs, A. Persoons, M. Samoc, B. Luther-Davies, A.C. Willis, submitted for publication.
[2] I.R. Whittall, A.M. McDonagh, M.G. Humphrey, M. Samoc, Adv. Organomet. Chem. 42 (1998) 291.
[3] I.R. Whittall, A.M. McDonagh, M.G. Humphrey, M. Samoc, Adv. Organomet. Chem. 43 (1998) 349.
[4] T. Verbiest, S. Houbrechts, M. Kauranen, K. Clays, A. Persoons, J. Mater. Chem. 7 (1997) 2175.
[5] I.R. Whittall, M.G. Humphrey, M. Samoc, J. Swiatkiewicz, B. Luther-Davies, Organometallics 14 (1995) 5493.
[6] I.R. Whittall, M.G. Humphrey, D.C.R. Hockless, B.W. Skelton, A.H. White, Organometallics 14 (1995) 3970.
[7] I.R. Whittall, M.G. Humphrey, A. Persoons, S. Houbrechts, Organometallics 15 (1996) 1935.
[8] A.M. McDonagh, I.R. Whittall, M.G. Humphrey, B.W. Skelton, A.H. White, J. Organomet. Chem. 519 (1996) 229.
[9] A.M. McDonagh, I.R. Whittall, M.G. Humphrey, D.C.R. Hockless, B.W. Skelton, A.H. White, J. Organomet. Chem. 523 (1996) 33.
[10] A.M. McDonagh, M.P. Cifuentes, I.R. Whittall, M.G. Humphrey, M. Samoc, B. Luther-Davies, D.C.R. Hockless, J. Organomet. Chem. 526 (1996) 99.
[11] I.R. Whittall, M.G. Humphrey, S. Houbrechts, A. Persoons, D.C.R. Hockless, Organometallics 15 (1996) 5738.
[12] I.R. Whittall, M.G. Humphrey, M. Samoc, B. Luther-Davies, Angew. Chem. Int. Ed. Engl. 36 (1997) 370.
[13] I.R. Whittall, M.P. Cifuentes, M.G. Humphrey, B. Luther-Davies, M. Samoc, S. Houbrechts, A. Persoons, G.A. Heath, D.C.R. Hockless, J. Organomet. Chem. 549 (1997) 127.
[14] I.R. Whittall, M.G. Humphrey, M. Samoc, B. Luther-Davies, D.C.R. Hockless, J. Organomet. Chem. 544 (1997) 189.
[15] R.H. Naulty, M.P. Cifuentes, M.G. Humphrey, S. Houbrechts, C. Boutton, A. Persoons, G.A. Heath, D.C.R. Hockless, B. Luther-Davies, M. Samoc, J. Chem. Soc. Dalton Trans. (1997) 4167.
[16] R.H. Naulty, A.M. McDonagh, I.R. Whittall, M.P. Cifuentes, M.G. Humphrey, S. Houbrechts, J. Maes, A. Persoons, G.A. Heath, D.C.R. Hockless, J. Organomet. Chem. 563 (1998) 137.
[17] A.M. McDonagh, M.G. Humphrey, M. Samoc, B. Luther-Davies, S. Houbrechts, T. Wada, H. Sasabe, A. Persoons, J. Am. Chem. Soc. 121 (1999) 1405.
[18] K.S. Kochar, B.S. Bal, R.P. Deshpande, S.N. Rajadhyaksha, H.W. Pinnick, J. Org. Chem. 48 (1983) 1765.
[19] S. Thorand, F. Vogtle, N. Krause, Angew. Chem. Int. Ed. Engl. 38 (1999) 3721.
[20] D. Touchard, P. Haquette, N. Pirio, L. Toupet, P.H. Dixneuf, Organometallics 12 (1993) 3132.
[21] I.R. Whittall, M.G. Humphrey, D.C.R. Hockless, Aust. J. Chem. 50 (1997) 991.
[22] I.R. Whittall, M.P. Cifuentes, M.G. Humphrey, B. Luther-Davies, M. Samoc, S. Houbrechts, A. Persoons, G.A. Heath, D. Bogsanyi, Organometallics 16 (1997) 2631.
[23] B. Chaudret, G. Commenges, R. Poilblanc, J. Chem. Soc. Dalton Trans. (1984) 1635.
[24] C.A. McAuliffe, R.V. Parish, P.D. Randall, J. Chem. Soc. Dalton Trans. (1979) 1730.
[25] M.I. Bruce, E. Horn, J.G. Matisons, M.R. Snow, Aust. J. Chem. 37 (1984) 1163.
[26] W.B. Austin, N. Bilow, W.J. Kelleghan, K.S.Y. Lau, J. Org. Chem. 46 (1981) 2280.
[27] Z. Otwinowski, W. Minor, in: C.W. Carter Jr., R.M. Sweet (Eds.), Methods in Enzymology, Academic Press, New York, 1997, p. 307.
[28] P. Coppens, in: F.R. Ahmed, S.R. Hall, C.P. Huber (Eds.), Crystallographic Computing, Munksgaard, Copenhagen, 1970, p. 255.
[29] S. Mackay, C.J. Gilmore, C. Edwards, N. Stewart, K. Shankland, maXus: Computer Program for the Solution and Refinement of Crystal Structures, Nonius, The Netherlands, MacScience, Japan, The University of Glasgow, UK, 1999.
[30] A. Altomare, M. Cascarano, C. Giacovazzo, A. Guagliardi, M.C. Burla, G. Polidori, M. Camalli, J. Appl. Crystallogr. 27 (1994) 425.
[31] P.T. Beurskens, G. Admiraal, G. Beurskens, W.P. Bosman, R. de Gelder, R. Israel, J.M.M. Smits, The DIRDIF-94 Program System, Technical Report of the Crystallography Laboratory, University of Nijmegen, Nijmegen, The Netherlands, 1994.
[32] M. Stahelin, D.M. Burland, J.E. Rice, Chem. Phys. Lett. 191 (1992) 245.
[33] K. Clays, A. Persoons, Rev. Sci. Instrum. 63 (1992) 3285.
[34] S. Houbrechts, K. Clays, A. Persoons, Z. Pikramenou, J.-M. Lehn, Chem. Phys. Lett. 258 (1996) 485.
[35] M. Sheik-bahae, A.A. Said, T. Wei, D.J. Hagan, E.W. van Stryland, IEEE J. Quantum Electron. 26 (1990) 760.